NEOPLASIA
www.neoplasia.com

Volume 10 Number 11 November 2008 pp. 1253–1258 1253

Mutation and Methylation Analysis of the *Chromodomain-Helicase-DNA Binding 5* Gene in Ovarian Cancer[1,2]

Kylie L. Gorringe[*], David Y.H. Choong[*], Louise H. Williams[*,†], Manasa Ramakrishna[*,†], Anita Sridhar[*], Wen Qiu[*,†], Jennifer L. Bearfoot[*,†] and Ian G. Campbell[*,†]

*Victorian Breast Cancer Research Consortium, Cancer Genetics Laboratory, Peter MacCallum Cancer Centre, East Melbourne, Victoria, Australia; †Department of Pathology, University of Melbourne, Melbourne, Victoria, Australia

Abstract

Chromodomain, helicase, DNA binding 5 (CHD5) is a member of a subclass of the chromatin remodeling Swi/Snf proteins and has recently been proposed as a tumor suppressor in a diverse range of human cancers. We analyzed all 41 coding exons of *CHD5* for somatic mutations in 123 primary ovarian cancers as well as 60 primary breast cancers using high-resolution melt analysis. We also examined methylation of the *CHD5* promoter in 48 ovarian cancer samples by methylation-specific single-stranded conformation polymorphism and bisulfite sequencing. In contrast to previous studies, no mutations were identified in the breast cancers, but somatic heterozygous missense mutations were identified in 3 of 123 ovarian cancers. We identified promoter methylation in 3 of 45 samples with normal *CHD5* and in 2 of 3 samples with *CHD5* mutation, suggesting these tumors may have biallelic inactivation of *CHD5*. Hemizygous copy number loss at *CHD5* occurred in 6 of 85 samples as assessed by single nucleotide polymorphism array. Tumors with *CHD5* mutation or methylation were more likely to have mutation of *KRAS* or *BRAF* ($P = .04$). The aggregate frequency of *CHD5* haploinsufficiency or inactivation is 16.2% in ovarian cancer. Thus, *CHD5* may play a role as a tumor suppressor gene in ovarian cancer; however, it is likely that there is another target of the frequent copy number neutral loss of heterozygosity observed at 1p36.

Neoplasia (2008) 10, 1253–1258

Introduction

Chromodomain helicase DNA-binding 5, CHD5, is a member of a subclass of the chromatin remodeling Swi/Snf proteins [1]. Proteins within this subclass contain a Swi-Snf–like helicase and two chromodomain motifs. Members of this protein class have been shown to be part of complexes that mediate chromatin remodeling and affect gene transcription. Recently, Bagchi et al. [2] identified *CHD5* as a putative tumor suppressor gene through functional analysis in a mouse model. The model suggested that partial *CHD5* deficiency compromises p53 signaling and therefore abrogation of CHD5 function might represent a generic mechanism for cancer development. Evidence that *CHD5* functions as a tumor suppressor in primary human cancers has come principally from studies of neuroblastoma where loss of the *CHD5* locus on chromosome 1p36.3 is very common [3]. CHD5 expression is consistently down-regulated in primary neuroblastomas and cell lines [4] and may be affected by methylation in neuroblastoma cell lines based on reexpression after treatment with 5-azacytidine [5].

To date, the only evidence for a broader role of *CHD5* in human cancer has come from a genome-wide breast and colon cancer genome sequencing study where *CHD5* was proposed as a "CAN-gene" [6]. Heterozygous missense mutations were identified in 2 of 24 primary breast cancers and 1 of 11 cell lines. Loss of heterozygosity

Abbreviations: CN, copy number; HRM, high-resolution melt; LOH, loss of heterozygosity

Address all correspondence to: Ian Campbell, Victorian Breast Cancer Research Consortium Cancer Research Laboratory, Peter MacCallum Cancer Centre, Locked Bag 1, A'Beckett St, Melbourne, VIC 8006, Australia. E-mail: ian.campbell@petermac.org

[1]This study was funded by the Victorian Breast Cancer Research Consortium, Australia. M.R. is a recipient of a Cancer Council of Australia Postgraduate Scholarship. W.Q. is a recipient of a National Health and Medical Research Council Dora Lush Postgraduate Scholarship. J.L.B. is a recipient of a University of Melbourne Research Scholarship.
[2]This article refers to supplementary materials, which are designated by Tables W1 to W3 and Figures W1 to W3 and are available online at www.neoplasia.com.
Received 26 June 2008; Revised 7 August 2008; Accepted 12 August 2008

DOI 10.1593/neo.08718

(LOH) at 1p is a common event in breast and ovarian cancers and has been shown to correlate with poor survival [7,8], and therefore, *CHD5* is a logical candidate for the target of this LOH in these cancer types. In this study, we have extended the range of tumors where *CHD5* plays a tumor suppressor role by demonstrating the existence of somatic mutations and methylation in primary epithelial ovarian cancers.

Materials and Methods

DNA Samples

One hundred and twenty-three primary ovarian cancers (56 serous, 20 mucinous, 34 endometrioid, and 13 other) were obtained from patients presenting to the hospitals in the south of England, UK. DNA for mutation and methylation analyses was extracted from whole fresh frozen specimens. Representative sections were hematoxylin and eosin–stained, and all tumors were assessed to contain >60% tumor epithelium. Normal DNA was extracted from matching peripheral blood samples. Matching tumor and normal DNA from 60 primary breast cancers was provided by the Peter MacCallum Cancer Centre tissue bank or by Dr Nick Hayward (Queensland Institute for Medical Research, Brisbane, Australia). This study was approved by institutional ethics committees. Before mutation screening, all stock DNA underwent whole genome amplification (WGA) using the Repli-G Phi-mediated amplification system (Qiagen, Hilden, Germany). To minimize the potential for generation of artifacts, WGA was carried out in triplicate, using 25 ng of primary DNA, and the products were pooled.

Mutation Analysis

The *CHD5* gene was analyzed by high-resolution melt (HRM). Exons 9, 13, 30, and 31 were amplified using previously reported primer sequences [6]. For the remaining exons, primers were designed to amplify each of the 41 exons and intron/exon boundaries of the coding sequence in 156- to 477-bp fragments (median, 202 bp). Primers were designed using the software packages ExonPrimer and Primer3 [9]. Primer sequences and amplification conditions are listed

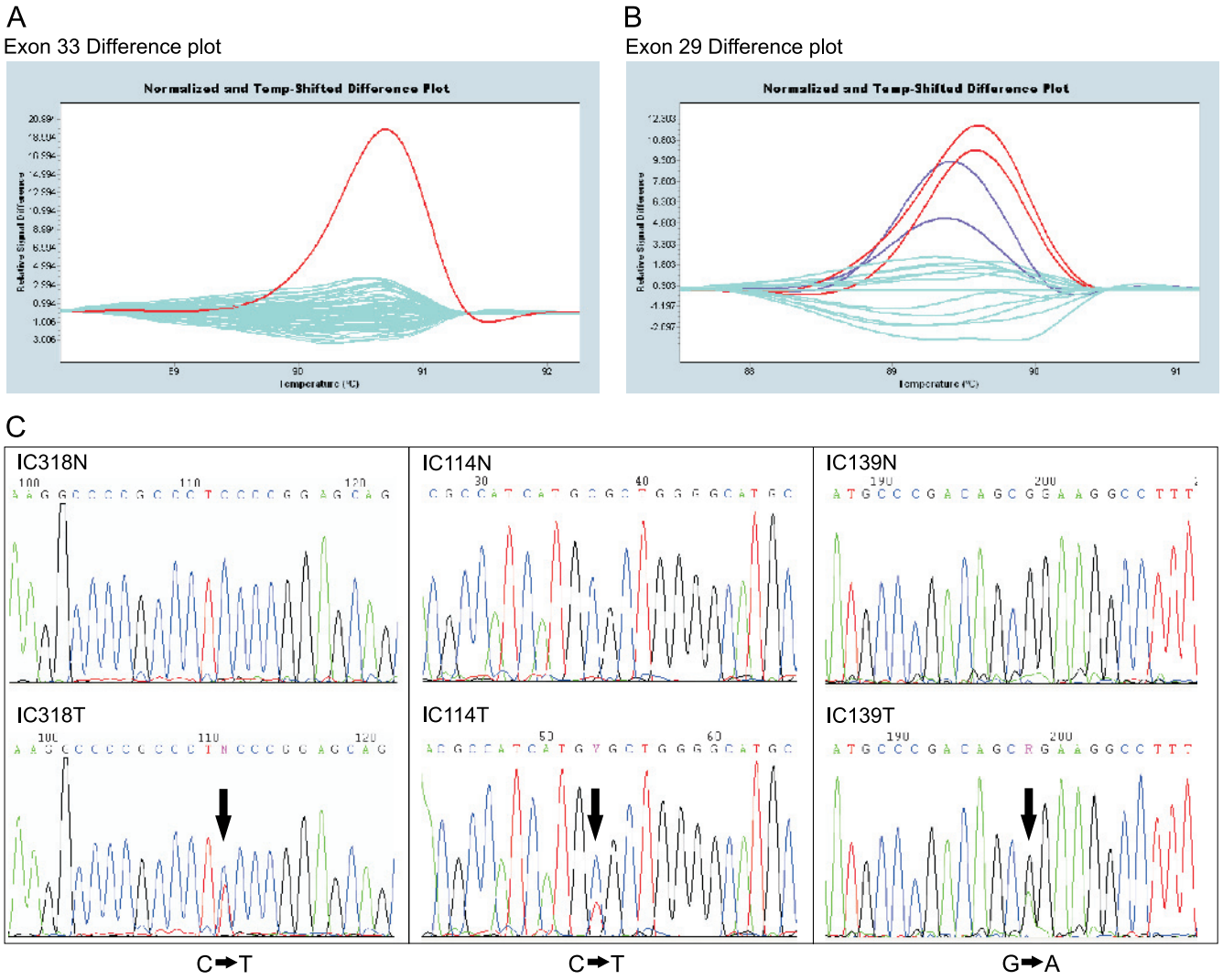

Figure 1. Somatic alterations in *CHD5*. (A) Somatic mutation in ovarian tumor IC318. The shift in exon 33 melting profile for IC318 is indicated in red. (B) Somatic mutations in exon 29. The melting profiles are shown for tumor samples IC114 (purple) and IC139 (red). (C) Normal and tumor sequence traces for exon 33 (left, arrow indicates C4992T heterozygous mutation) and exon 29 (center, arrow indicates C4412T; and right, arrow indicates G4386A).

in Table W1. Owing to their larger size, exons 5, 10, 11, 15, 23, and 38 were amplified in two overlapping fragments. *TP53* (exons 5-8), *KRAS* (amino acids 1-36), and *BRAF* (V600E) were analyzed previously [10] or using HRM (Table W1). High-resolution melt was carried out in duplicate using polymerase chain reaction (PCR) products amplified from 10 ng of WGA template DNA. Gene scanning analyses were carried out for each exon using the LightCycler 480 (Roche Diagnostics, Mannheim, Germany). Samples with replicated shifts in the DNA melt curves were reamplified, and the PCR product was directly sequenced using BigDye Terminator v3.1 (Applied Biosystems, Foster City, CA). Somatic alterations were confirmed by resequencing from the unamplified stock tumor DNA and the matching normal DNA. Polymerase chain reaction products for sequencing were purified by nucleotide removal columns or agarose gel extraction (Qiagen).

Analysis of CpG Island Methylation by Methylation-Specific Single-Stranded Conformation Polymorphism and Bisulfite Sequencing

The *CHD5* CpG island was identified in University of California Santa Cruz genome browser (genome.ucsc.edu) and methylation-specific single-stranded conformation polymorphism (MS-SSCP) PCR primers designed from genomic DNA sequence using MethPrimer (www.urogene.org/methprimer) [11]. Both forward and reverse oligonucleotide primers were fluorescently labeled with either FAM or HEX. Primer sequences are listed in Table W1.

DNA samples were treated with bisulfite using the MethylEasy Kit (Human Genetic Signatures, Sydney, Australia) following the manufacturer's instructions. After PCR amplification, products were analyzed by SSCP using the ABI 3130 Genetic Analyzer (Applied Biosystems) as described previously [12]. Samples showing a shift in mobility were sequenced, whereas the remainder were considered normal. Twenty-four samples were sequenced without performing SSCP. *Sss*I methylase–treated normal DNA was used as a positive control for CpG island methylation. This enzyme methylates all CpGs before bisulfite treatment. Polymerase chain reaction products for sequencing were reamplified using unlabeled primers and purified by nucleotide removal columns (Qiagen). Purified PCR products were sequenced in both forward and reverse directions using BigDye Terminator v3.1 (Applied Biosystems). Full methylation at a particular CpG was defined as follows: >60% of the average bisulfite sequencing signal was "C," whereas partial methylation was 40% to 60%. "Methylation-positive" was defined as at least 18 of the 35 CpGs within the PCR product showing full or partial methylation. "Partial methylation" was defined as at least 6 of 35 CpGs showing full or partial methylation.

Real-time Reverse Transcription Quantitative PCR

RNA was extracted from cell lines or from microdissected tumors using the miRVana RNA isolation kit according to the manufacturer's instructions (Ambion, Austin, TX). Samples were reverse transcribed and amplified according to the Affymetrix Gene 1.0ST array protocol (Affymetrix, Santa Clara, CA) and 30 ng of the ssDNA was used per 10-μl PCR. This RNA amplification step was performed to ensure sufficient template in the reaction for reproducible quantitation. Primers were designed to *CHD5* and a control gene *PGK1* (Table W1), and PCR was performed with the SYBRgreen QPCR mix (ThermoScientific, Waltham, MA) and the LightCycler 480 (Roche Diagnostics, Mannheim, Germany). Cp ("crossing point") was calculated using the second derivative maximum method. The relative levels of expression of *CHD5* and *PGK1* were calculated using a normal ovarian surface epithelial cell line (HOSE) RNA as a control standard curve.

Single Nucleotide Polymorphism Array Analysis

Affymetrix single nucleotide polymorphism (SNP) 500K and SNP 6.0 Mapping arrays were performed on unamplified DNA obtained from microdissected fresh frozen tissue sections, and the data were analyzed using Partek Genomics Suite (Partek, St Louis, MO), GTYPE (Affymetrix), and CNAG software as described previously [13]. Loss of heterozygosity was determined by examination of the allele-specific copy number (CN) ratios in CNAG [14,15].

Results and Discussion

Mutation Analysis of CHD5 *Using HRM*

High-resolution melt analysis covering all of the *CHD5* protein coding sequence and intron/exon boundaries (a total of 47 PCR products) was carried out on DNA from 123 primary ovarian cancers and 60 primary breast cancers. No mutations were identified in any of the breast tumors, but three ovarian tumors were shown to harbor somatic heterozygous missense alterations: C4992T (Ser1631Phe), C4412T (Arg1438Cys) and G4386A (Arg1429Gln) (Figure 1 and Table 1). The somatic nature of the mutations was confirmed by sequencing matching normal lymphocyte DNA. The Ser1631Phe and Arg1429Gln mutations were identified in grade 3, stage III serous type tumors, and the Arg1438Cys mutation was identified in a grade 2 stage IA endometrioid tumor. Analysis of the effect of the missense mutations on protein structure and function was performed using

Table 1. *CHD5* Coding Sequence Alterations.

Exon	Sequence Alteration	Codon	Amino Acid	Heterozygote Frequency	
				Breast Cancer	Ovarian Cancer
Somatic mutations					
29	G4386A	CGG to CAG	Arg1429Gln	0/60	1/121
29	C4412T	CGC to TGC	Arg1438Cys	0/60	1/121
33	C4992T	TCC to TTC	Ser1631Phe	0/60	1/123
Polymorphisms					
4*	G529C	CTG to CTC	Leu143Leu	7/60	13/123
5	G679C	CGG to CGC	Arg193Arg	0/60	1/122
6	C876G	TCC to TGC	Ser259Cys	1/60	0/123
7*	C1003T	TTC to TTT	Phe301Phe	27/60	41/123
7	G1014A	AGC to AAC	Ser305Asn	1/60	0/123
8*	A1204G	GTA to GTG	Val368Val	22/60	39/123
9	C1378A	GGC to GGA	Gly426Gly	2/60	0/123
10	T1666C	CAT to CAC	His521His	0/60	1/123
11	C1768T	TAC to TAT	Tyr556Tyr	1/60	0/123
12*	C1957T	TAC to TAT	Tyr619Tyr	9/60	15/123
14	G2200A	CTG to CTA	Leu700Leu	1/60	0/123
15*	C2479T	AAC to AAT	Asn793Asn	13/60	21/123
16*	T2593C	ATT to ATC	Ile831Ile	24/60	51/123
18	G2878A	CCG to CCA	Pro926Pro	0/60	1/123
22*	G3436A	GCG to GCA	Ala1112Ala	9/60	13/123
28	C4336T	CTC to CTT	Leu1412Leu	3/60	4/123
31*	T4715C	TCG to CCG	Ser1539Pro	30/60	53/121
32	G4828T	ATG to ATT	Met1576Ile	1/60	0/123
34	C5089T	TCC to TCT	Ser1663Ser	0/60	1/123
35	C5170T	GAC to GAT	Asp1690Asp	0/65	1/123
36	C5344T	ATC to ATT	Ile1748Ile	0/60	1/123
36	C5349T	ACG to ATG	Thr1750Met	1/60	0/123

Asterisks indicate previously identified polymorphisms.

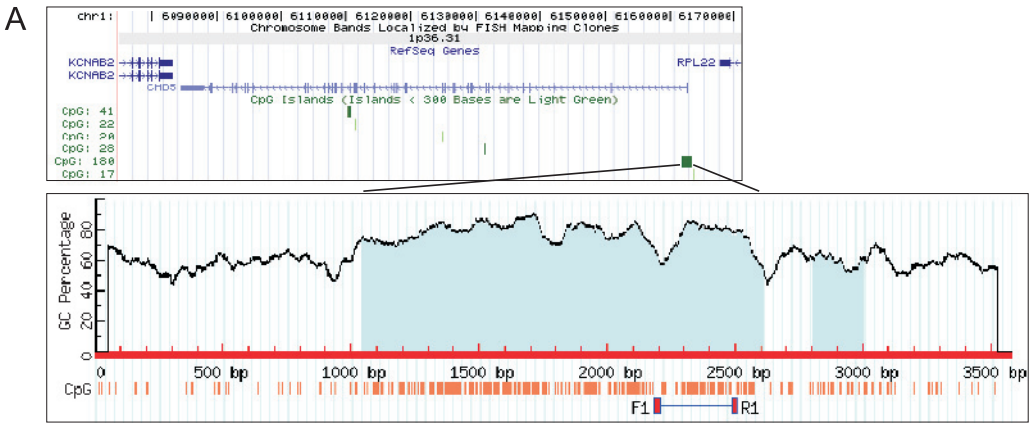

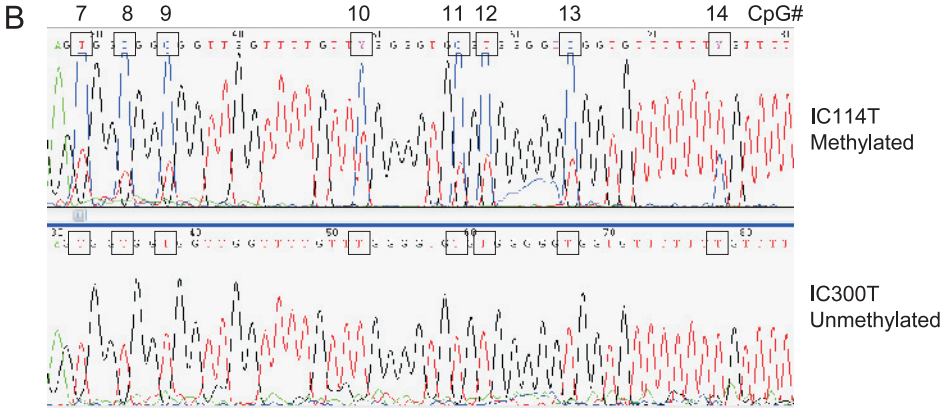

C

Sample	CpG Number 1	2	3	4	5	6	7	8	9	10	11	12	13	14	15	16	17	18	19	20	21	22	23	24	25	26	27	28	29	30	31	32	33	34	35
HEY	■	■	■	■	■	■	■	■	■	■	■	■	■		■	■	▒	■	■	■	■	■	■	■	■	■	■				■	■	■		
JAM	■	■	■	■	■	■	■	■	■	■	■	■	■	▒	■	■	▒	■	■	■	■	■	■	■	■	■	■	▒	■	■	■	■	■	▒	■
OVCA-432	■	■	■	■	■	■	■	■	■	■	■	■	■	▒	■	■	▒	■	■	■	■	▒	■	■	■	■	■	■	▒	■	□	▒	▒	▒	■
IC197T	■	■	■	■	■	■	■	■	■	▒	▒	▒	□	□	□	□	□	□	▒	□	□	□	▒	■	■	■	■	■	■	■	■	■	■	▒	▒
IC139T	▒	■	■	■	■	■	■	■	■	▒	▒	▒	■	■	□	▒	▒	■	▒	▒	▒	■	■	■	■	■	■	■	■	■	■	■	▒	▒	□
IC114T	■	■	▒	■	■	■	■	■	■	■	■	■	■	□	□	□	□	□	□	□	□	□	□	▒	□	▒	□	□	▒	▒	▒	▒	□	□	▒
IC50T	▒	□	▒	□	□	■	■	■	■	▒	□	□	▒	▒	▒	■	▒	■	■	■	▒	■	■	■	■	■	■	■	■	■	▒	■	■	▒	▒
IC80T	▒	▒	□	▒	▒	▒	■	■	▒	□	▒	□	▒	▒	▒	▒	□	□	▒	□	□	▒	▒	■	■	■	■	□	□	▒	▒	□	□	□	□
IC70T	■	□	□	■	■	▒	▒	■	■	□	□	□	▒	□	▒	▒	□	□	□	□	□	□	□	□	□	□	□	□	□	□	□	□	□	□	□
IC71T	□	□	□	□	□	□	■	■	■	□	□	■	□	□	■	▒	□	□	□	□	□	□	□	■	■	■	■	□	□	□	□	□	□	□	□
IC95T	□	□	□	□	□	□	□	□	□	▒	▒	▒	□	□	□	□	□	□	□	□	□	□	□	□	□	□	▒	□	□	□	□	□	□	□	□
IC14T	□	□	□	□	□	□	□	▒	▒	□	□	□	□	□	□	□	□	□	□	□	□	□	□	□	□	□	□	□	□	□	□	□	□	□	□
IC151T	□	□	□	□	□	□	□	□	□	□	▒	□	■	□	□	□	□	□	□	□	□	□	□	□	□	□	□	□	□	□	□	□	□	□	□
IC520T	□	□	■	□	□	□	□	□	□	■	□	□	□	□	□	□	□	□	□	□	□	□	□	□	□	□	□	□	□	□	□	□	□	□	□
IC2T	□	□	□	□	□	□	□	□	□	□	□	□	□	□	□	□	□	□	□	□	□	□	□	□	□	□	□	□	□	□	▒	▒	■	□	□

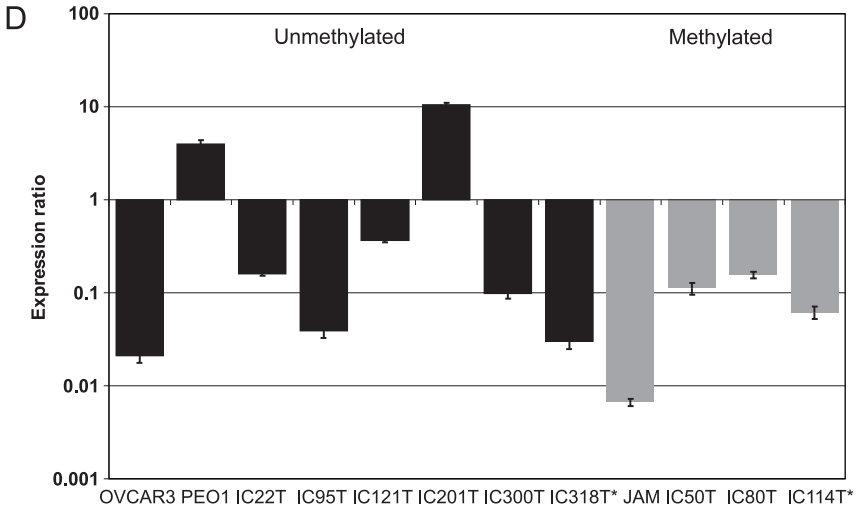

three different prediction algorithms: PolyPhen [16], SIFT [17], and PMUT [18]. All three mutations were predicted to affect protein function by at least two of the prediction algorithms (Table W2).

The absence of somatic mutations in 60 primary breast cancers is at variance with the 9% mutation frequency (2/24 primary breast cancers and 1/11 breast cancer cell lines) reported by Sjöblom et al. [6] in a genome-wide sequencing screen. It is unlikely that the absence of somatic mutations in the breast cancers is caused by lack of sensitivity of HRM, which has a growing reputation as a highly sensitive mutation detection technique [19,20]. We were able to detect a large number of polymorphisms located in the coding sequence (22 variants) or within the intron sequences (24 variants; Table 1, Table W3, and Figure W1). In our hands, sequence variants were readily detectable even in samples where there was normal DNA contamination or where the variant was present at a low abundance due to LOH (Figure W1). In addition, we were able to detect compound polymorphisms, in which a sample with a common polymorphism also had a less frequent polymorphism present (Figure W1). The distribution of histologic subtypes, grade, and stage of tumors examined in our study and by Sjöblom et al. [6] was similar, suggesting that the discrepancy in tumor mutation frequency might be due to chance given that it was not statistically significant (Fisher's exact test, $P = .079$). Our study does suggest that the frequency of *CHD5* mutations in breast cancers might be lower than the 9% reported previously and highlights the importance of following up leads from genome-wide sequencing screens with independent sample sets. This is the first study of somatic mutation and methylation of *CHD5* in ovarian cancer, and the data indicate that *CHD5* has a tumor suppressor role in a subset of cases. Interestingly, all three mutations were detected in tumors that were heterozygous across the *CHD5* locus.

The CHD5 *Promoter Is Sometimes Methylated in Primary Ovarian Cancer*

Because the expression of tumor suppressor genes is sometimes reduced as a consequence of promoter hypermethylation, we examined the promoter of *CHD5* in ovarian tumors. *CHD5* has a predicted CpG island spanning 1577 bp, beginning 631 bp upstream of the transcription start site and comprising 180 CpGs (Figure 2). Methylation was detected in three of six ovarian cancer cell lines, with at least 80% of CpGs fully methylated as determined by bisulfite sequencing (Figure 2). Primary ovarian cancers showed less frequent methylation, with 5 of 48 methylated and 2 of 48 partially methylated. We verified that methylation was not the result of contamination of tumor by fibroblasts or lymphocytes by bisulfite sequencing the *CHD5* promoter in one cancer-associated fibroblast cell line, one microdissected stromal DNA sample, and one normal lymphocyte DNA sample. None of these samples showed any methylation. Promoter methylation was more frequent and extensive in the cell lines than the primary tumors, suggesting that methylation of the *CHD5* promoter may be common in the transition from primary tumor to cell line. Notably, two methylated samples (IC114T and IC139T) also carried somatic mutations (Table 2). We carried out real-time reverse transcription PCR for *CHD5* on samples for which sufficient RNA could be extracted. Samples with methylated promoters showed uniformly low levels of expression (Figure 2). Unmethylated samples showed variable expression levels, suggesting that there may be other mechanisms by which *CHD5* expression is regulated. The three *CHD5* wild type cancers with a high level of promoter methylation comprised a mixed mullerian tumor and two mucinous tumors.

Table 2. Summary of *CHD5* and Pathway Interactions.

Sample	Subtype	*CHD5*	*KRAS Mut*	*KRAS* CN	*BRAF Mut*	*TP53 Mut*
IC114	Endometrioid	Arg1438Cys, methylation	wt	—	wt	wt
IC139	Serous	Arg1429Gln, methylation	wt	—	V600E	wt
IC318	Serous	Ser1631Phe	wt	Gain	wt	wt
IC197	MMT	Methylation	wt	—	wt	wt
IC50T	Mucinous	Methylation	wt	n	V600E	wt
IC80T	Mucinous	Methylation	G12V	n	wt	wt
IC281	Serous	CN loss	wt	n	wt	—
IC288	Serous	CN loss	wt	n	wt	—
IC382	Serous	CN loss	wt	n	wt	—
IC594	Endometrioid	CN loss	wt	n	wt	wt
P0566	Mixed	CN loss	wt	n	wt	wt
P5338	Serous	CN loss	—	Gain	—	—
IC022	Serous	CN gain	wt	Gain	wt	Y220C
IC135	Serous	CN gain	wt	n	wt	del156-159
IC434	Endometrioid	CN gain	wt	n	wt	wt

(—) indicates not done; *n*, normal CN; *wt*, wild type.

Copy Number Loss Is an Alternate Mechanism of CHD5 *in Ovarian Cancer*

A mouse model of CHD5 deficiency suggested that haploinsufficiency of *CHD5* may contribute to cancer progression rather than a "two-hit" mechanism expected of a classic tumor suppressor [2]. In light of this, we considered the possibility that *CHD5* might be the target of CN loss, which would be consistent with (but not proof of) targeted haploinsufficiency of *CHD5*. We evaluated 85 primary ovarian cancers (56 with known *CHD5* mutation status) using Affymetrix 500K or 6.0 SNP Mapping arrays [13]. These arrays are able to detect both CN losses and CN neutral LOH. We detected

Figure 2. *CHD5* promoter methylation in ovarian cancer. (A) University of California Santa Cruz genome browser view of the *CHD5* gene, which is located on the reverse strand (genome.ucsc.edu). The *CHD5* promoter contains a strong CpG island as demonstrated in the MethPrimer (www.urogene.org/methprimer) output below. The location of the primers used for SSCP and sequencing is shown (F1 and R1). (B) Sequence electropherogram traces from primary ovarian tumors showing methylated and unmethylated samples. (C) Summary of bisulfite sequencing from cell lines and primary tumors showing methylation. CpG dinucleotide number within the PCR product listed across the top from distal to proximal relative to transcription start site. Black, fully methylated (>60%); gray, partial methylation (40-60%); white, <40% methylation. An additional 15 tumors were sequenced that showed no methylation. Samples with a *CHD5* mutation are shown in bold. Sample IC139T data are based on cloning the PCR product and sequencing five clones as the direct sequencing was poor. (D) Quantitative PCR of *CHD5*. The expression level of *CHD5* is shown as a ratio relative to the control gene. An asterisk indicates a *CHD5*-mutated sample. SEs are shown.

CHD5 CN loss (defined as a $\log_2$ ratio of <−0.3) [13] in 6 (7%) and gain ($\log_2$ ratio of >0.3) in 3 (3.5%) of 85 ovarian tumors (Figure W2). The *CHD5* region showed LOH (both CN neutral and CN loss) in 30 samples (35%); however, LOH at any locus on chromosome 1p was detected in 39 samples (46%) and suggests that another gene(s) is the target of LOH on chromosome 1p (Figure W3).

The mouse and *in vitro* models of *CHD5* gene dosage suggested that CHD5 acts within the p53 pathway, with loss of CHD5 resulting in reduced expression of p53 target genes. *CHD5* loss also interacted with *KRAS* to promote transformation. We therefore looked to see whether *CHD5* mutation or methylation coincided with alterations in the KRAS pathway or *TP53* mutation. Interestingly, three of six of the *CHD5* mutation- or methylation-affected samples had alteration in the *KRAS* pathway, one by *KRAS* mutation and two by *BRAF* mutation (P = .04, Fisher's exact test), whereas none had mutation of *TP53* (Table 2). However, this association was not evident among the samples showing *CHD5* CN loss only with none from five samples having either *KRAS* or *BRAF* mutation (P = 1, Fisher's exact test).

Altogether, when mutation (2.4%) and methylation (without mutation, 6.7%) are combined, *CHD5* is affected in 9.1% of ovarian cancers, which is extended to 16.2% if cases with CN loss (7.1%) are included. However, the consequence of heterozygous CN loss at *CHD5* in ovarian cancer is not clear, given that two of three samples with mutation also showed methylation, suggesting biallelic inactivation rather than haploinsufficiency. Our study supports the contention that *CHD5* is a tumor suppressor gene in a subset of ovarian tumors. The disparity between the frequency of *CHD5* alteration (16%) and LOH at 1p (46%) strongly suggests another tumor suppressor gene in the region. *CHD5* mutation and/or methylation, but not CN loss, may co-operate with the KRAS pathway in tumorigenesis; however, the number of samples is small and this result will require future validation. The lack of *CHD5* mutations in the breast cancer samples screened in this study is in contrast to the 9% frequency reported previously [6]. Because the difference in mutation frequencies is not statistically significant, it is likely to be due to chance, although a contribution of the screening methodologies used cannot be excluded.

References

[1] Marfella CG and Imbalzano AN (2007). The Chd family of chromatin remodelers. *Mutat Res* **618**, 30–40.

[2] Bagchi A, Papazoglu C, Wu Y, Capurso D, Brodt M, Francis D, Bredel M, Vogel H, and Mills AA (2007). CHD5 is a tumor suppressor at human 1p36. *Cell* **128**, 459–475.

[3] White PS, Thompson PM, Gotoh T, Okawa ER, Igarashi J, Kok M, Winter C, Gregory SG, Hogarty MD, Maris JM, et al. (2005). Definition and characterization of a region of 1p36.3 consistently deleted in neuroblastoma. *Oncogene* **24**, 2684–2694.

[4] Okawa ER, Gotoh T, Manne J, Igarashi J, Fujita T, Silverman KA, Xhao H, Mosse YP, White PS, and Brodeur GM (2008). Expression and sequence analysis of candidates for the 1p36.31 tumor suppressor gene deleted in neuroblastomas. *Oncogene* **27**, 803–810.

[5] Thompson PM, Gotoh T, Kok M, White PS, and Brodeur GM (2003). *CHD5*, a new member of the chromodomain gene family, is preferentially expressed in the nervous system. *Oncogene* **22**, 1002–1011.

[6] Sjöblom T, Jones S, Wood LD, Parsons DW, Lin J, Barber TD, Mandelker D, Leary RJ, Ptak J, Silliman N, et al. (2006). The consensus coding sequences of human breast and colorectal cancers. *Science* **314**, 268–274.

[7] Ragnarsson G, Eiriksdottir G, Johannsdottir JT, Jonasson JG, Egilsson V, and Ingvarsson S (1999). Loss of heterozygosity at chromosome 1p in different solid human tumours: association with survival. *Br J Cancer* **79**, 1468–1474.

[8] Bernardini M, Lee CH, Beheshti B, Prasad M, Albert M, Marrano P, Begley H, Shaw P, Covens A, Murphy J, et al. (2005). High-resolution mapping of genomic imbalance and identification of gene expression profiles associated with differential chemotherapy response in serous epithelial ovarian cancer. *Neoplasia* **7**, 603–613.

[9] Rozen S and Skaletsky H (2000). Primer3 on the WWW for general users and for biologist programmers. *Methods Mol Biol* **132**, 365–386.

[10] Foulkes WD, Englefield P, and Campbell IG (1994). Mutation analysis of RASK and the "FLR exon" of NF1 in sporadic ovarian carcinoma. *Eur J Cancer* **30A**, 528–530.

[11] Li LC and Dahiya R (2002). MethPrimer: designing primers for methylation PCRs. *Bioinformatics* **18**, 1427–1431.

[12] Williams LH, Choong D, Johnson SA, and Campbell IG (2006). Genetic and epigenetic analysis of CHEK2 in sporadic breast, colon, and ovarian cancers. *Clin Cancer Res* **12**, 6967–6972.

[13] Gorringe KL, Jacobs S, Thompson ER, Sridhar A, Qiu W, Choong DY, and Campbell IG (2007). High-resolution single nucleotide polymorphism array analysis of epithelial ovarian cancer reveals numerous microdeletions and amplifications. *Clin Cancer Res* **13**, 4731–4739.

[14] Nannya Y, Sanada M, Nakazaki K, Hosoya N, Wang L, Hangaishi A, Kurokawa M, Chiba S, Bailey DK, Kennedy GC, et al. (2005). A robust algorithm for copy number detection using high-density oligonucleotide single nucleotide polymorphism genotyping arrays. *Cancer Res* **65**, 6071–6079.

[15] Liu W, Xie CC, Zhu Y, Li T, Sun J, Cheng Y, Ewing CM, Dalrymple S, Turner AR, Sun J, et al. (2008). Homozygous deletions and recurrent amplifications implicate new genes involved in prostate cancer. *Neoplasia* **10**, 897–907.

[16] Sunyaev S, Ramensky V, Koch I, Lathe W III, Kondrashov AS, and Bork P (2001). Prediction of deleterious human alleles. *Hum Mol Genet* **10**, 591–597.

[17] Ng PC and Henikoff S (2001). Predicting deleterious amino acid substitutions. *Genome Res* **11**, 863–874.

[18] Ferrer-Costa C, Gelpi JL, Zamakola L, Parraga I, de la Cruz X, and Orozco M (2005). PMUT: a Web-based tool for the annotation of pathological mutations on proteins. *Bioinformatics* **21**, 3176–3178.

[19] Reed GH and Wittwer CT (2004). Sensitivity and specificity of single-nucleotide polymorphism scanning by high-resolution melting analysis. *Clin Chem* **50**, 1748–1754.

[20] Krypuy M, Ahmed AA, Etemadmoghadam D, Hyland SJ, DeFazio A, Fox SB, Brenton JD, Bowtell DD, and Dobrovic A (2007). High resolution melting for mutation scanning of TP53 exons 5-8. *BMC Cancer* **7**, 168.

Table W1. Oligonucleotide Primer Sequences.

Primer Name	Primer Sequence (5′–3′)	Annealing Temperature (°C)	Primer Concentration (nM)	Buffer*	Length (bp)
CHD5Exon1Fnew	CAGCGCACGGGTTAAGG	65	300	Q	161
CHD5Exon1Rnew	CGCTCACCTGACATCTCGT				
CHD5Exon2F	AGTAACTGCTGCCACCTTCTG	62	200	Q	217
CHD5Exon2R	CAGATGCAGCCACAACCC				
CHD5Exon3F	CTCTGTTGCCCTCACTGTCC	65	200	Q	287
CHD5Exon3R	CATACAGGCAAGAGGCTCAG				
CHD5Exon4F	CAACTCTACCTCTGGCCTGG	58	200	SM	202
CHD5Exon4R	GGTACCACCAGAGGATGTGC				
CHD5Exon5_1F	TCTCATCTCACCTGGCCTTG	60	300	SM	209
CHD5Exon5_1R	GATGGTGACCGTCTCTACAGC				
CHD5Exon5_2F	AGTTCAGCGCCAACAACC	58	200	Q	195
CHD5Exon5_2R	GACTAGGTGCCCACCCAAC				
CHD5Exon6F	TGGTTGGCTATCATCACTGC	58	200	Q	195
CHD5Exon6R	ATGCAAATGCACACACACG				
CHD5Exon7F	CTGGGATCACAGGACCC	56	200	Q	186
CHD5Exon7R	GCCAAGAACTCTCTGGAAGG				
CHD5Exon8F	AGGACTTCCATGACTGCCTC	62	300	Q	272
CHD5Exon8R	CCAAATGAGGGCACAGGG				
CHD5Exon9newF	CCCTGTGCCCTCATTTGG	58	300	Q + QS	477
CHD5Exon9newR	CTTTGCGGGATCGGCTAC				
CHD5Exon10_1F	CACCTTGGGGACCCTTC	56	200	SM	193
CHD5Exon10_1R	TGCCCACTTGACAAAGAACTC				
CHD5Exon10_2F	CCTTCATGGTGGGGCTG	65	200	Q	171
CHD5Exon10_2R	TAGCACAGCCACCCTCCC				
CHD5Exon11_1F	CCCTTCTGTGACTTTGTGCC	54	100	Q	184
CHD5Exon11_1R	GCTCCTCCATCTTGGCATAG				
CHD5Exon11_2F	CTACGGCTCTGGGGATGAAG	58	200	Q	196
CHD5Exon11_2R	AGAAGCTGACGTGGCCC				
CHD5Exon12F	GCGACCCACATCTGTTCAC	68	300	SM	197
CHD5Exon12R	CAGCCTGTGCCTAGCAGC				
CHD5Exon13Fnew	CCTTGCTCACCTGCCTCCAAT	58	300	Q	216
CHD5Exon13Rnew	CCCCTGCACATTCAAGTCTGAG				
CHD5Exon14F	CGTGTCTGAACCGCTGC	60	200	Q	262
CHD5Exon14R	AGGACCAGCCACCCCTC				
CHD5Exon15_1F	AGGTGGTCTCACGGCATC	54	100	Q	176
CHD5Exon15_1R	TTCTCCCGAATCACCGAG				
CHD5Exon15_2F	GAACGCGAGTTTGAGATGTG	54	100	Q	184
CHD5Exon15_2R	GGGCCTTCCTACCGTCC				
CHD5Exon16F	TGTGATCCGCTCTGCTCC	58	300	SM	227
CHD5Exon16R	GGAAGCTCTGGGGTCTGG				
CHD5Exon17F	CTGACAGGCCCCACTCTC	62	100	Q	185
CHD5Exon17R	ACCACCACCTCCCTAGCC				
CHD5Exon18F	CTGGCTGTTATCCCAGCTT	60	300	SM	274
CHD5Exon18R	GAATCGACCCAGGAGACCA				
CHD5Exon19F	GTCTGACCCAGCCTGCC	62	100	Q	224
CHD5Exon19R	ATGGCGGTCATGGAGAAG				
CHD5Exon20F	CCTTTGGTGCAGAGTCAGAG	58	200	Q	261
CHD5Exon20R	ATCAGGGCAGGATGCTCTC				
CHD5Exon21F	CCTTGCTCCTTGGCAGTTC	56	200	Q	191
CHD5Exon21R	AATCAGAACCCTTGGGCAG				
CHD5Exon22F	CCCCAAACACTCCCATCTG	60	300	Q	233
CHD5Exon22R	AAGGACAGAACCTGCCTGAG				
CHD5Exon23_1F	GAGCCACGGGTGCTGAG	60	300	SM	200
CHD5Exon23_1R	GTCATGGACCCCGACTTG				
CHD5Exon23_2F	AGGAGCGCATCACGCAG	65	200	Q + M	183
CHD5Exon23_2R	CCACGCTCCCTCGGAAC				
CHD5Exon24F	CTGCACCAGTGCTTTCCTTC	60	300	SM	188
CHD5Exon24R	ACCTGGTCGGAGGAGGAG				
CHD5Exon25F	GTCCTCACACTGCATTTGCC	68	300	Q	283
CHD5Exon25R	TGGAAGGCGTGGACACAG				
CHD5Exon26F	GGAGGGCAGAGATGGCTC	65	200	Q + M	260
CHD5Exon26R	GTGAGGGGCACCAGTCC				
CHD5Exon27Fnew	GGAAGTATGTGGGCCATTGTC	58	300	SM	352
CHD5Exon27Rnew	GAGCCCAGAGATTCCTGATCC				
CHD5Exon28F	CTCCCACCTGAGGAACTGTG	62	200	Q	167
CHD5Exon28R	GAAGCAGGGGCAGAAAGAG				
CHD5Exon29F	CTGTCCTGGGCTCATACTCC	68	300	SM	222
CHD5Exon29R	CTACTCAGGGGCAGGTGGTC				
CHD5Exon30Fnew	GATGGTTGAAGATCAGCCAGG	58	300	Q + QS	334
CHD5Exon30Rnew	CTCTGACCACTGACCCACAAG				
CHD5Exon31Fnew	CAAGCCTGTGACACTTTCAGC	58	300	Q	358
CHD5Exon31Rnew	TCTGTGGGATTGTGGGTTAGAC				

Table W1. (*continued*)

Primer Name	Primer Sequence (5′–3′)	Annealing Temperature (°C)	Primer Concentration (nM)	Buffer*	Length (bp)
CHD5Exon32F	ACCTGTCTCAGCTCTTTCCC	65	200	Q	156
CHD5Exon32R	CACCCCACACACACCACAG				
CHD5Exon33F	CCCAGGCCTTGTAGTTCTCC	62	200	Q	211
CHD5Exon33R	AGACATGGCACTGGGGTG				
CHD5Exon34F	GTTTTCTGGGACCCCACC	62	100	Q	172
CHD5Exon34R	GGGGCACAGGTAGAGAACAC				
CHD5Exon35F	GATGGATGAATGAATGTGATCTG	54	100	Q	211
CHD5Exon35R	AGGAAGCCTCAGCTCTCTGC				
CHD5Exon36F	CACTTCTCACCCTGCTCACC	65	300	SM	187
CHD5Exon36R	GAACGGGCAAGTCCCTG				
CHD5Exon37F	CAGGTTTGCCCTTAATGGTG	58	200	Q	218
CHD5Exon37R	CTCCTGACACCGTCCCTC				
CHD5Exon38_1F	ACGGAGGGTAGCCATTCAG	54	200	Q	182
CHD5Exon38_1R	GGCGAGGCACTCCACTTC				
CHD5Exon38_2F	ACCTGAACATGACGCAGGAC	56	100	Q	227
CHD5Exon38_2R	GCCCTCATCTACAGCCAAGAG				
CHD5Exon39F	CATCCCTGCATCCTACCATC	65	300	Q	266
CHD5Exon39R	ACCCAGCCTCCACCCAG				
CHD5Exon40F	CCACCTGTGAAGCTGAGTCC	58	100	Q	184
CHD5Exon40R	CACCCGTGTGCATGCTG				
CHD5Exon41F	CTATGTGACCGGTAGGTGCC	58	300	Q	185
CHD5Exon41R	CAGCAGCCCTCACCTCAG				
KRAS 1-36F	GGCCTGCTGAAAATGACTGA	65	100	SM	162
KRAS 1-36R	GTCCTGCACCAGTAATATGC				
P53 Exon5F	CACTTGTGCCCTGACTTTCA	60	100	SM	267
P53 Exon5R	AACCAGCCCTGTCGTCTCT				
P53 Exon6F	CAGGCCTCTGATTCCTCACT	60	100	SM	185
P53 Exon6R	CTTAACCCCTCCTCCCAGAG				
P53 Exon7F	CCTGCTTGCCACAGGTCT	60	100	SM	201
P53 Exon7R	GTGTGCAGGGTGGCAAGT				
P53 Exon8F	TTTCCTTACTGCCTCTTGCTTC	60	100	SM	227
P53 Exon8R	TAACTGCACCCTTGGTCTCC				
BRAF V600E_F	CCTAAACTCTTCATAATGCTTGCTC	65	100	SM	189
BRAF V600E_R	CCACAAAATGGATCCAGACA				
CHD5 Meth F	GTTGTTTTGAAGATTTTGTTTT	58	100	Q + M	321
CHD5 Meth R	CTAATTACTATAACAACCCCATCCC				
CHD5 QPCR F	CTCAACGAGCCCTTCAAGTC	60	300	S	97
CHD5 QPCR R	CTGCTCCAGCAGCTTAAACC				
PGK1 F	ATTAGCCGAGCCAGCCAAAATAG	60	50	S	94
PGK1 R	TCATCAAAAACCCACCAGCCTTCT				

*Buffer: Q = Qiagen Hotstar *Taq* with 1.5 mM $MgCl_2$; Q + M = Qiagen Hotstar *Taq* with 3.5 mM $MgCl_2$; Q + QS = Qiagen Hotstar *Taq* with 1.5 mM $MgCl_2$ and 1× "Q" solution; S, SYBR green mix from ThermoScientific; SM = Roche ScanMaster mix with 2.5 mM $MgCl_2$.

Table W2. Predicted Effect of Amino Acid Missense Substitutions.

Sequence Change	PolyPhen*	SIFT†	PMUT‡	Consensus
This study				
Arg1429Gln	**1.892**	**0.00**	0.34/3	Pathogenic
Arg1438Cys	**2.792**	**0.00**	**0.81/6**	Pathogenic
Ser1631Phe	**1.666**	**0.05**	**0.67/3**	Pathogenic
Previous mutations§				
Val45Met	0.675	0.14	0.04/9	Neutral
Asp119Met	**2.025**	**0.04**£	0.36/2	Pathogenic
Arg667Gly	1.321	0.26	0.49/0	Neutral

Samples in bold were scored as possibly pathogenic.
*PolyPhen: scores increase from zero with a higher score being more likely to be pathogenic.
†SIFT: scores ≤0.05 classed as pathogenic.
‡PMUT: first score increases from zero, pathogenic if >0.5, second score measures reliability from 0 being unreliable to 9 being very reliable.
§From Sjöblom et al. [6].
£SIFT flagged this change as unreliable because only one other sequence had this amino acid for comparison.

Table W3. Intron Polymorphisms.

Intron*	Sequence Alteration	Frequency	
		Breast Cancer	Ovarian Cancer
2	+30 T/G	5/60	4/123
3	+33 C/A	10/60	13/123
4	+33 C/T	0/60	1/123
6	+18 T/C	0/60	1/123
8*	+40 C/A	7/60	9/123
8*	+46 C/A	1/60	0/123
14	+10 C/T	0/60	1/123
15	+10 C/G	0/60	2/123
15*,†	−18 T/C	24/60	51/123
15*,†	−26 T/C	24/60	51/123
18	+21 G/A	2/60	0/123
18	+27 G/A	1/60	0/123
19	+13 G/A	0/60	1/123
19*	−28 A/C	20/60	25/121
22*	+49 G/A	22/60	28/123
24*	+13 C/T	24/60	39/123
24	+27 G/T	0/60	1/123
25*	+61 delC	2/60	0/123
27	+69 C/T	1/59	0/123
30*	−25 T/C	35/58	71/119
34	−5 G/A	2/60	1/123
37	+29 delC	30/60	54/123
39	+29 G/A	0/60	1/123
39	+41 G/A	0/60	1/123

*Asterisks indicate previously identified polymorphisms.
†The two-intron 15 polymorphisms are tightly linked with the exon 16 T2593C polymorphism.

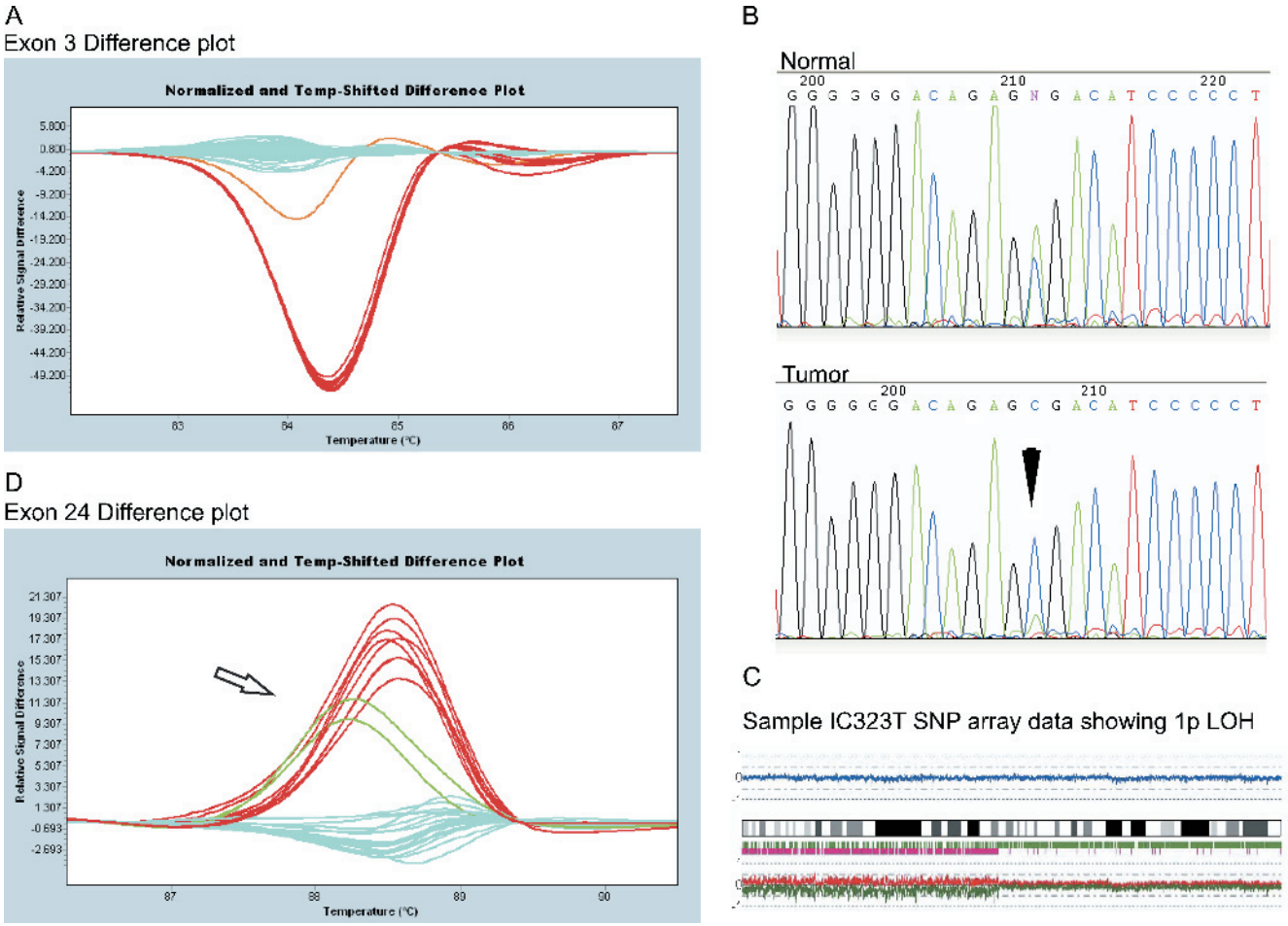

Figure W1. Sensitivity of HRM to detect sequence alterations. (A) Exon 3 polymorphism difference plot showing the polymorphism shift in red and a tumor sample, IC323, which has LOH of the polymorphism in orange. (B) Sequence traces with the normal IC323 sequence showing intron 3 +33C/A polymorphism and the tumor IC323 sequence showing LOH of the "A" allele (filled arrowhead). (C) The CN neutral LOH was confirmed by the SNP array data. (D) Intron 24 compound polymorphism. In red are samples heterozygous for the single intron 24 +13C/T polymorphism, whereas in green (open arrow) is the sample heterozygous for both +13C/T and +27G/T polymorphisms.

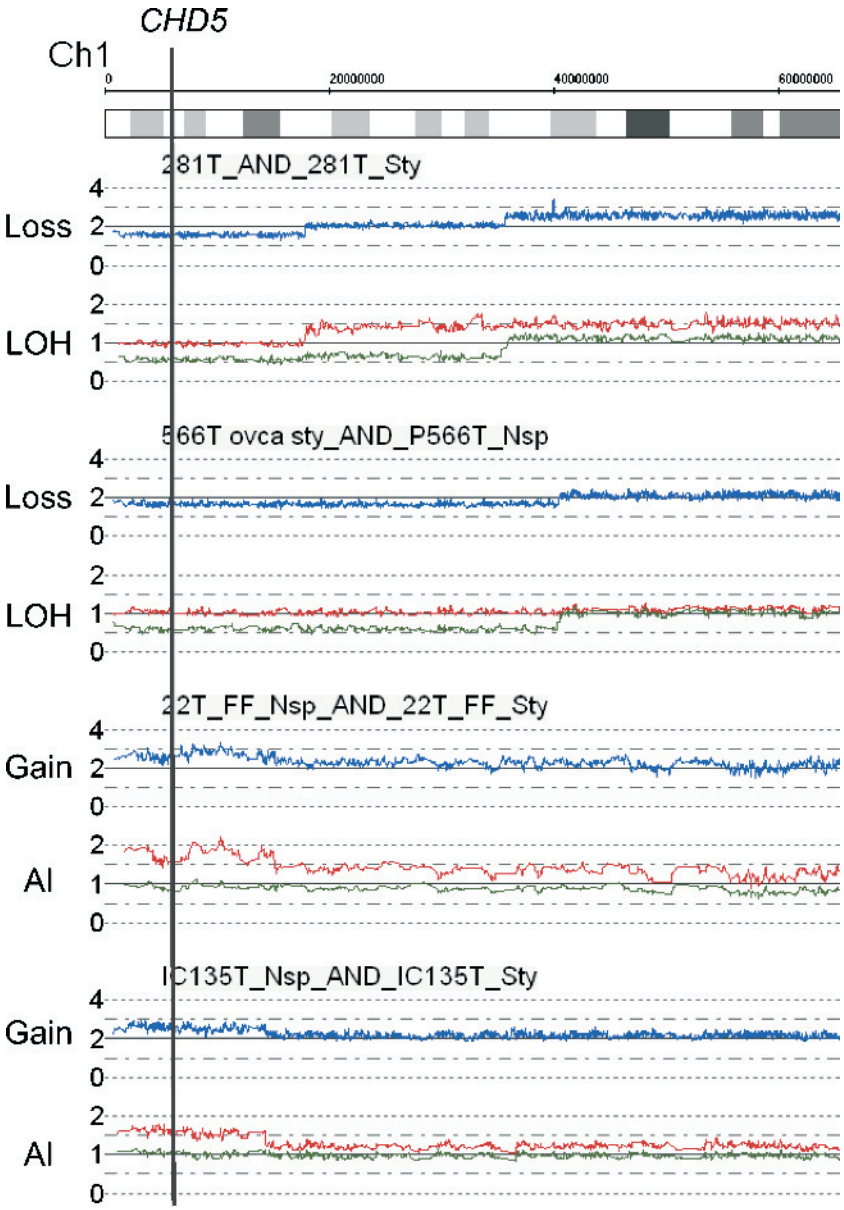

Figure W2. SNP array data for chromosome 1p. Example data from four primary ovarian tumors, two with CN loss and LOH at *CHD5* and two with CN gain and allelic imbalance (AI) at *CHD5*. Blue line is a 10-point moving average, with the scale indicating linear CN. Below is the allele-specific CN for the most intense (red line) and least intense (green line) alleles.

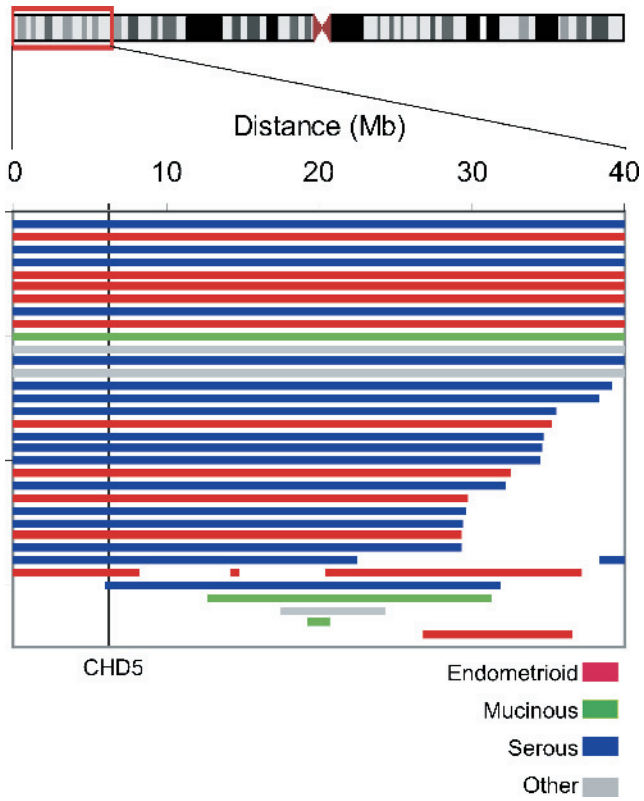

Figure W3. Chromosome 1p LOH in ovarian cancer samples. SNP array data from p-terminus at left to 1p34.2 at right. Bar indicates presence of LOH, color coded to histologic subtype as indicated by the legend. The location of *CHD5*, affected in 30 (35%) of 85 samples, is shown.